Experimental and theoretical studies of the (C $1s^{-1},\pi^*)^3\Pi$ state of CO: Momentum transfer dependence and vibrational structure

J. T. Francis
Department of Chemistry, McMaster University, Hamilton, Ontario L8S 4M1, Canada

N. Kosugi
Institute for Molecular Science, Myodaiji, Okazaki 444, Japan

A. P. Hitchcock
Department of Chemistry, McMaster University, Hamilton, Ontario L8S 4M1, Canada

(Received 26 July 1994; accepted 29 August 1994)

The intensity of the $X\ ^1\Sigma^+ \rightarrow (C\ 1s^{-1},\pi^*)^3\Pi$ transition of CO has been measured by electron energy loss spectroscopy using a range of scattering angles (0°–45°) and impact energies (376 to 1806 eV) in order to investigate the momentum transfer dependence of a spin forbidden inner-shell excitation. A Franck–Condon factor analysis of the vibrational structure of the singlet and triplet $(C\ 1s^{-1},\pi^*)$ states was used to quantify differences in the potential energy curves of these states. *Ab initio* self-consistent field configuration interaction (SCF-CI) calculations were carried out to generate the potential curves of the $^1\Pi$ and $^3\Pi(C\ 1s^{-1},\pi^*)$ states. The electronic and vibrational energies and Franck–Condon factors are in good agreement with the experimental results. The calculations indicate that the difference in the $^1\Pi$ and $^3\Pi$ potential curves are related to differences in relaxation of both the (active) π^* and other (passive) valence electrons. © *1994 American Institute of Physics.*

I. INTRODUCTION

The vast majority of all work in the field of inner shell excitation via electron impact techniques has been conducted under conditions of small momentum transfer, which effectively simulates photoabsorption. (A bibliography of atomic and inner shell excitation studies has been published recently.[1]) Such conditions are achieved experimentally by employing small scattering angles ($\theta<2°$) and "fast" electrons, typically using impact energies of more than five times the excitation energy of the core level transition. As the momentum transfer becomes significant (large θ and/or small impact energy), the probability of nondipole transitions increases. The ability to excite electric dipole forbidden processes represents a distinct advantage of electron impact techniques, specifically electron energy loss spectroscopy (EELS), over photoabsorption.

Dipole forbidden spin exchange excitations to inner shell excited states are difficult to study on account of their intrinsically small cross sections. The first reported observation was that of Shaw *et al.* in 1982 who detected the vibrationally resolved $X\ ^1\Sigma_g \rightarrow (1\sigma_g^{-1},\pi_u^1)^3\Pi_u$ transition in N_2.[2] Such spin forbidden transitions are induced by lowering the impact energy close to the energy of excitation. Under these slow collision conditions the probability of exchange of incident and target electrons becomes appreciable. The $(C\ 1s^{-1},\pi^*)^3\Pi$ state of CO has been studied previously by Ungier and Thomas,[3] Shaw *et al.*,[4] and Harrison and King.[5] Recently we have investigated the $(C\ 1s^{-1},\pi^*)$ triplet state spectroscopy of CO, benzene, ethylene and acetylene.[6]

To date there has been no systematic study of the angular dependence of inelastic cross sections for a spin-forbidden inner-shell excitation. Harrison and King investigated the impact energy dependence of the singlet–triplet intensity ratio of CO but mainly using a fixed 90° scattering angle and impact energies less than 40 eV above threshold.[5,7] In order to explore more fully the spin exchange scattering mechanism we have measured the energy loss spectrum of CO in the region of the $(C\ 1s^{-1},\pi^*)^3\Pi$ and $^1\Pi$ states using a wide range of angles (2°–45°) and impact energies (376–1806 eV). These results have been analyzed to examine the momentum transfer dependence of the triplet/singlet intensity ratios.

In addition, the vibrational band structure of both the $^1\Pi$ and $^3\Pi(C\ 1s^{-1},\pi^*)$ states has been measured and analyzed. High quality *ab initio* calculations have been carried out to determine the potential curves and thus Franck–Condon overlap factors for the $(C\ 1s^{-1},\pi^*)^3\Pi$ and $^1\Pi$ states. The theoretical calculations are in good agreement with the present experimental results, with high resolution photoabsorption studies of the $C\ 1s \rightarrow {}^1\Pi$ transition,[8–12] and with an earlier EELS experimental study of the $C\ 1s \rightarrow {}^3\Pi$ transition[4] in CO. Small differences in the potential curves of the $^1\Pi$ and $^3\Pi(C\ 1s^{-1},\pi^*)$ states are explained in terms of differences in the relaxation of both the active π^* and passive valence electrons in the core excited states.

II. EXPERIMENT

The inner shell electron energy loss spectra (ISEELS) were recorded using a newly developed, variable impact energy, variable angle, high-resolution electron spectrometer which will be described in detail in a future publication. Briefly, a monochromated electron beam impinges on the gas target. Electrons inelastically scattered at a mechanically determined scattering angle (−10° to 110°) are dispersed using a lens system and a hemispherical electron energy analyzer. The signal is detected using a channel electron multiplier and standard pulse counting electronics. In this study, spectra were recorded using a jet formed by expansion through a capillary array (100:1 aspect ratio of the channels). The jet was found to eliminate background contributions from secondary electron scattering which had been a problem when a gas cell was used.

Constant residual energy (90 to 1520 eV above threshold) scanning was used which is advantageous since it eliminates chromatic aberrations at the analyzer exit lens as the spectrum is scanned. A resolution of 0.18 eV was used to study the vibrational band structure. The resolution was degraded to 0.40 eV to study the angle and impact energy dependence of the $^3\Pi$ and $^1\Pi$ intensity in order to improve signal statistics. Count rates were as little as 2 cps at higher scattering angles (45°) which necessitated long acquisition times (24–48 h).

III. CALCULATIONS

The calculations were carried out using the GSCF3 code[13,14] on a MIPS RS3330 UNIX workstation. The core-ionized and core-excited self-consistent field Hartree–Fock (SCF-HF) solutions were obtained with explicit consideration of the core hole. Potential energy curves for the $^1\Sigma^+$ ground state, the $^2\Sigma^+(C\ 1s^{-1},\pi^*)$ ionized state, and the $^1\Pi$ and $^3\Pi(C\ 1s,\pi^*)$ core excited states were obtained with the configuration interaction (CI) method using the SCF orbitals as in Ref. 15. The vibrational states and the Franck–Condon factors were obtained from numerical solutions of the nuclear Schrödinger equation.[16] Cooley's method[17] was used in the numerical integration.

The CI calculations allow double substitution to the virtual-orbital space from the valence-orbital space ($C\ 2s$, $C\ 2p$, $O\ 2s$, and $O\ 2p$). The valence space is described with single substitution within the π-electron subspace and the core space is frozen. The virtual and vacant valence orbitals were obtained with the hole (V^{N-1}) potential method.[18] Primitive basis functions were taken from (73/6) contracted Gaussian-type functions of Huzinaga *et al.*[19] They were augmented with single polarization functions (ζ_d=0.600 for C, 1.154 for O). The contraction schemes were (51121/411/1*) and (721/51/1*) for carbon and oxygen atoms, respectively.

IV. RESULTS AND DISCUSSION

A. Momentum transfer dependence of the triplet–singlet intensity ratio

Figure 1 presents $C\ 1s$ spectra of CO in the region of excitation to the $(C\ 1s^{-1},\pi^*)^3\Pi$ and $(C\ 1s^{-1},\pi^*)^1\Pi$ states, recorded at small scattering angles (<4°) and residual electron energies of 90, 105, and 1520 eV, corresponding to impact energies at the $^3\Pi$ excitation of 376, 391, and 1806 eV. The solid lines passing through the experimental data points in Fig. 1 are the results of curve fits using Voigt lineshapes for each of the vibrational components. The Lorentzian width was set to 60 meV (the natural linewidth[11,12]) while the Gaussian width was optimized, yielding a value of 180 meV which was the same as the experimental resolution determined from the fwhm of the $^1S_0 \rightarrow {}^1P_1$ transition in He at 21.22 eV. Figure 1 also plots the ratio of the triplet to the singlet intensity, determined from spectra recorded at angles below 5°, as a function of fractional energy above threshold, $(E-E_{\mathrm{th}})/E_{\mathrm{th}}$, where E is the impact energy and E_{th} is the threshold energy. Figure 1 illustrates the "turning on" of the exchange between the incident and the target electron and thus excitation of the $^3\Pi$ state as the impact energy approaches threshold.

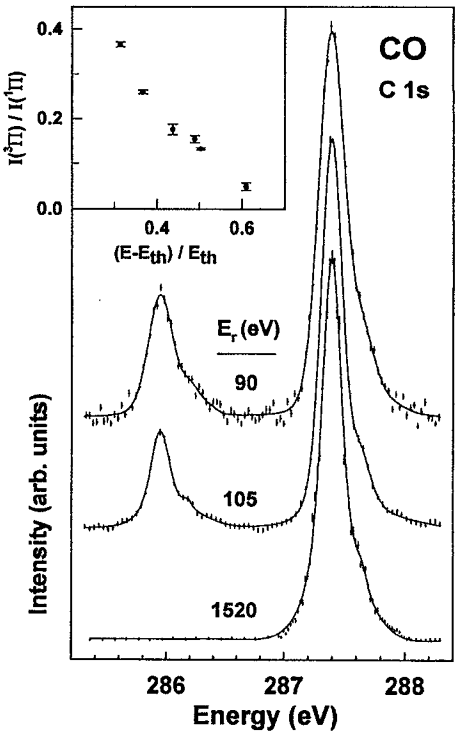

FIG. 1. Electron energy loss spectra of CO in the region of the $(C\ 1s^{-1},\pi^*)$ $^3\Pi$ and $^1\Pi$ states recorded at residual energies of 90, 105, and 1520 eV and scattering angles of 4°, 4°, and 2°, respectively. The resolution was 0.18 eV (FWHM). The insert plots the ratio of the triplet/singlet intensities as a function of fractional energy above threshold $[(E-E_{\mathrm{th}})/E_{\mathrm{th}}]$.

Figure 2 plots $C\ 1s$ spectra of CO recorded with 140 eV residual energy at scattering angles of 4°, 26°, and 45°. The insert to Fig. 2 presents a larger sampling of the variation of the triplet–singlet intensity ratio as a function of scattering angle. The peak areas used to evaluate the intensity ratios plotted in Figs. 1 and 2 were obtained from the curve fit procedure described above. The error bars were estimated from the counting statistics.

While the relative probability of triplet state excitation increases relatively rapidly above 10°, there is very little variation in the triplet/singlet intensity ratio at small angles (2° to 10°), at the impact energy used (426 eV). This behavior contrasts that found for many valence excited states, where large variations in the inelastic cross sections often occur in the 2°–10° range of scattering angles. The angle independence of the core excitation spectrum in the small angle regime is associated with the fact that K^2 is almost independent of angle whenever $\theta < \theta_E$ (where $\theta_E = \Delta E/2E$, in radians). θ_E is 20° for E=400 eV and ΔE=286 eV. Thus it is not surprising that K^2 increases by only a small amount for angles between 2°–10° (6.4 to 6.9 a.u.$^{-2}$) but by a much

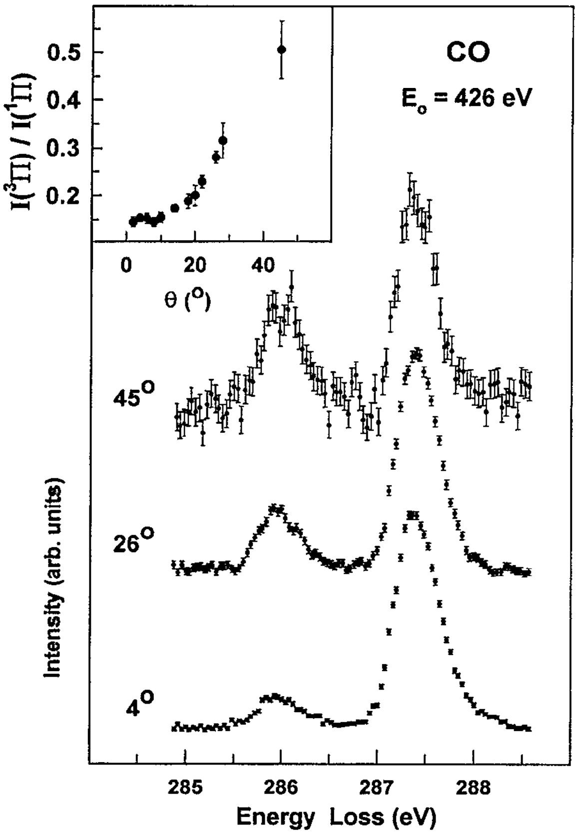

FIG. 2. Electron energy loss spectra of CO recorded using 140 eV residual energy and the indicated scattering angles. The insert plots the ratio of the $(C\ 1s^{-1},\pi^*)$ triplet/singlet intensities over 2°–45° scattering angle.

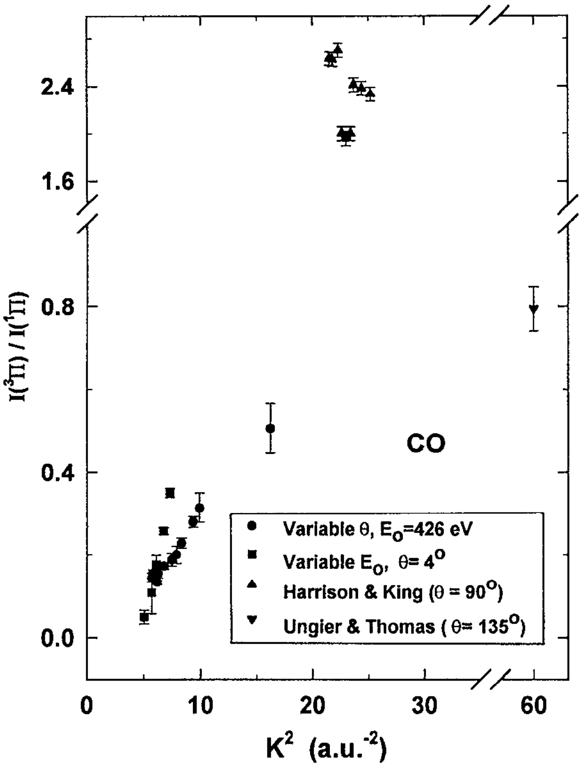

FIG. 3. Momentum transfer dependence of the $(C\ 1s^{-1},\pi^*)$ triplet/singlet intensity ratio derived from both variable impact energy and variable angle measurements. Literature data from Ungier and Thomas (Ref. 3) and Harrison and King (Ref. 5) are also included.

larger amount for a similar variation in angle at a larger average angle—for example, K^2 varies from 7.3 to 10.6 a.u.$^{-2}$ between 20°–30° at 400 eV impact energy.

Figure 3 combines the angle and impact energy dependence of the singlet–triplet intensity ratio by plotting this ratio as a function of momentum transfer. In addition to our data, results from Harrison and King[5] and Ungier and Thomas[3] are also plotted. Note that the four sets of results do not form a single smooth curve. Of particular note is the systematic deviation in the K^2 variation of the triplet-singlet intensity ratio when K^2 is changed by varying the impact energy rather than varying the scattering angle.

At impact energies near threshold the interaction between the incident electron and the target is large. Under these conditions the weak interaction assumption that is the basis of the first Born approximation[20,21] is likely to fail. A standard experimental test for the validity of the Born approximation is to measure the dependence on impact energy of the spectral intensities or intensity ratios at a fixed K^2. A necessary condition for applicability of the Born approximation is that the result is independent of impact energy. The data shown in Fig. 3 indicates that the transition intensity at a given K^2 does depend on the impact energy in the near threshold regime. Thus we conclude that the generalized oscillator strength concept[20,21] is inapplicable under near-threshold electron scattering conditions.

The intensity of the $^3\Pi$ signal, and thus the exchange probability, increases rather dramatically as the impact energy approaches the excitation threshold (see Fig. 1). Harrison and King have determined triplet–singlet intensity ratios of greater than 2 for impact energies less than 40 eV above threshold.[7] The measurements of Ungier and Thomas were carried out at an even larger K^2 (60 a.u.$^{-2}$) but, even at this very large momentum transfer, the triplet–singlet intensity ratio is only 0.80. Clearly, it is extremely low impact energies and not large scattering angles which are most important in spin forbidden excitations.

A naive view of the origin of the triplet spin-exchange signal is that at low energies the incident or outgoing electron can physically exchange with one of the target electrons. If this exchange is a completely random event with equal probability for exchanging electrons of the same or opposite spin, then the largest possible triplet–singlet intensity ratio would be 1.0. The observation of low impact energy spectra with a $^3\Pi/^1\Pi$ intensity ratio much greater than 1 (Ref. 7) clearly rules out this picture. The exchange process involved in the triplet excitation cannot be described by a simple 1:1 statistical exchange. Rather there must be selectivity in the interaction which favors exchange of unlike electrons when low energy electrons are involved. Alternatively, if one adopts a more state-oriented viewpoint, the limiting $^3\Pi/^1\Pi$ intensity ratio might be expected to be 3, reflecting the inherent state degeneracies. The Harrison and King results do not rule out this situation.

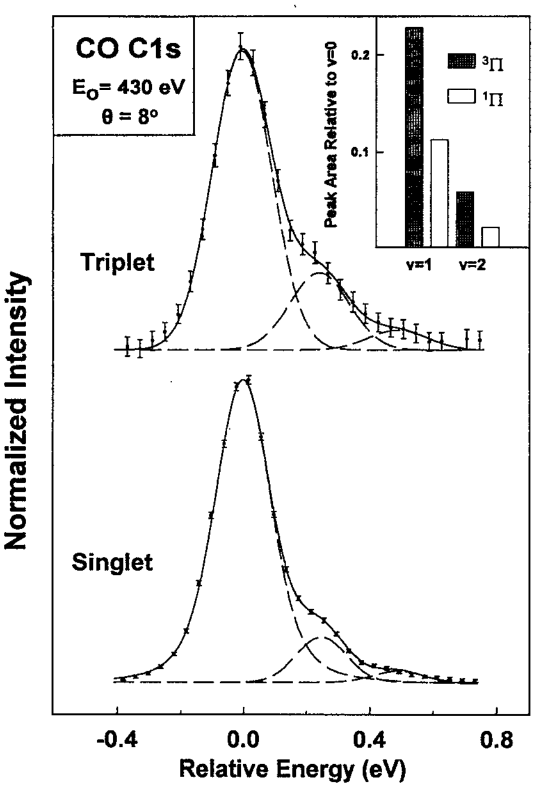

FIG. 4. Curve fit analysis of the vibrational band structure of the $X\ ^1\Sigma^+ \rightarrow (C\ 1s^{-1},\pi^*)\ ^3\Pi$ and $X\ ^1\Sigma^+ \rightarrow (C\ 1s^{-1},\pi^*)\ ^1\Pi$ transitions recorded at 140 eV residual energy, 8° scattering angle and 0.18 eV FWHM resolution. Details of the curve fit procedure are given in the text.

B. Vibrational structure of the $(C\ 1s^{-1},\pi^*)$ singlet and triplet states

Figure 4 presents a detailed lineshape analysis of the vibrational structure of the singlet and triplet features recorded at 0.18 eV FWHM energy resolution. The insert plots the intensities of the $v=1$ and $v=2$ components ratioed to that of the $v=0$ component. The peak intensities and positions derived from curve fitting are summarized in Table I in comparison to the results of the *ab initio* calculations.

Figure 5 presents the calculated anharmonic potential curve, in comparison to that derived from the experimental energies and Franck–Condon factors in an harmonic approximation. (Note that each of the theoretical curves have been shifted 0.5 eV to lower energy). The bond length of the core excited states are assumed to be longer than that in the ground state since the character of these transitions is essentially nonbonding to antibonding. Relative to the ground state, the shift in the equilibrium bond length derived from the Franck–Condon factors is 0.036 Å for the $^3\Pi$ state and 0.024 Å for the $^1\Pi$ state.

The separation of the adiabatic $(v=0)$ transitions is 1.47(3) eV, in good agreement with the values reported by others.[3–6] Analysis of the areas of the vibrational features reveals a difference in the Franck–Condon factors between the triplet and singlet states. This difference was also found in the high resolution study of Shaw *et al.*[2] The Franck–Condon factors and vibrational spacings for the $^3\Pi$ and $^1\Pi$ states are summarized in Table I, in comparison with the theoretical results. These results probe the differences in the potential energy surfaces of the triplet and singlet $(C\ 1s^{-1},\pi^*)$ excited states. The calculated equilibrium bond length of 1.1539 Å for the $^1\Pi$ state is similar to the value of 1.1527 Å estimated from our experimental Franck–Condon factor and the value of 1.153 Å reported by Domke *et al.*[8] Shaw *et al.* analyzed their results[4] to indicate a *reduction* of 0.024 Å in the equilibrium bond length of the $^1\Pi$ state relative to that of the $X\ ^1\Sigma^+$ ground state. We believe this is not consistent with the antibonding character of the π^* orbital.

The triplet state is predicted by the calculation to be slightly elongated at 1.1595 Å, somewhat less than the experimental estimate of 1.1639 Å. The calculated vibrational spacings are 268 meV (2162 cm^{-1}) and 245 meV (1980 cm^{-1}) for the singlet and triplet states, respectively, in reasonable agreement with experiment (250 and 242 meV). Experimentally, there are not enough resolved vibrational bands to make a reliable estimate of the anharmonicity of the potential curve of either state. Thus, the experimental observations have been represented in Fig. 5 by harmonic estimations of the true potential curves. The favorable agreement with theory supports our assumption that the bond length in the $^1\Pi$ and $^3\Pi$ states is larger than in the ground state as was also concluded by Domke *et al.*[8] for the $^1\Pi$ state.

The situation for the lowest valence $A\ ^1\Pi$ and $a\ ^3\Pi$ states is different than that just described for the core excited states. *Ab initio* SCF-CI calculations of the potential curves for the $A\ ^1\Pi$ and $a\ ^3\Pi$ states reported by Cooper and Langhoff[22] predict a slight contraction of the triplet state bond length (by ca. 0.03 Å) relative to the singlet state. The difference in the valence excitation energies $(T_{0\text{-}0})$, from both theory and experiment[22–25] is ca. 2.1 eV compared to 1.47(3) eV for the core excited states. The larger triplet–singlet splitting in the valence $\pi \rightarrow \pi^*$ excitation may be associated with better overlap between the initial and final states in the valence transition matrix element relative to that for the $1s \rightarrow \pi^*$ core excitation matrix element.

The general trends in the experimental observations are reproduced by the theoretical calculations although there are quantitative differences between experiment and theory. The equilibrium bond length and harmonic vibrational frequency calculated for the ground state are in agreement with the experimental results[25] within the errors in the doubly excited CI calculations using the double ζ plus polarization basis set. However they are worse than the result of a sophisticated calculation based on the complete active space (CAS) multiconfigurational SCF and contracted CI methods (1.129 Å, 273 meV).[26] The calculated $1s \rightarrow \pi^*$ excitation energies are about 0.45 eV larger than the experimental values, but the singlet–triplet separation and the calculated ionization energy are in good agreement with the experimental values. The equilibrium bond length of the $(C\ 1s^{-1})$ ionized state calculated in the present work (1.0906 Å) is slightly larger than the experimental estimate from $(C\ 1s^{-1}$, Rydberg) photoabsorption [1.073–1.083 Å (Ref. 8)]; $(C\ 1s^{-1})$ photoionization [1.077 Å (Ref. 9)]; and the theoretical result by Correia *et al.* [1.073 Å (Ref. 26)]. Ågren *et al.*[27] calculated the potential energy curve of the $(C\ 1s^{-1})$ ionized state based on

TABLE I. Experimental and theoretical results for potential curves and vibrational parameters.

$X\ ^1\Sigma^+$ (ground) state	Theory	Experiment	Expt. (Ref. 25)	
Bond length (r_e, Å)	1.1362	1.1283[a]	1.1283	
ω_e (eV)	0.281	0.269[a]	0.269	
$(C\ 1s^{-1},\pi^*)\ ^3\Pi$ state	Theory	Experiment[b]	Expt. (Ref. 4)	
$T_{0\text{-}0}$ (eV)	286.37	285.95 (5)	285.945 (5)	
ω_e (eV)	0.245	0.242 (6)	0.249(10)	
R_e (Å)	1.1595	1.1639	···	
$\Delta(v0-v1)$ (eV)	0.2549	0.242 (6)[c]	0.249(10)	
$\Delta(v0-v2)$ (eV)	0.5191	0.474(16)		
$\Delta(v0-v3)$ (eV)	0.7714			
Franck–Condon factors:				
$v0$	0.726	0.778(16)	0.80	
$v1$	0.218	0.177(16)	0.20	
$v2$	0.047	0.045 (6)	···	
$v3$	0.009	···	···	
$(C\ 1s^{-1},\pi^*)\ ^1\Pi$ state	Theory	Experiment[b]	Expt. (Ref. 4)	Expt. (Ref. 8)
$T_{0\text{-}0}$ (eV)	287.87	287.40[d]	287.40 (3)	287.400(2)
ω_e (eV)	0.268	0.248 (7)	0.258 (4)	0.256(2)
R_e (Å)	1.1539	1.1527	1.104 (2)	1.153
$\Delta(v0-v1)$ (eV)	0.2700	0.248 (7)	0.258	0.256(4)
$\Delta(v0-v2)$ (eV)	0.5418	0.500(19)	0.510	0.512(4)
$\Delta(v0-v3)$ (eV)	0.8068	···	···	0.768
Franck–Condon factors:				
$v0$	0.850	0.881	0.875	
$v1$	0.128	0.100 (3)	0.111 (3)	
$v2$	0.020	0.019 (9)	0.014 (1)	
$v3$	0.003	···		
$(C\ 1s^{-1})\ ^2\Sigma^+$ ion state	Theory	Experiment	Expt. (Ref. 9)	
$T_{0\text{-}0}$ (eV)	296.21	296.24[e]	296.13 (3)	
ω_e (eV)	0.292	···	0.309(17)	
R_e (Å)	1.0906	···	1.077 (5)	
$\Delta(v0-v1)$ (eV)	0.3084	···	0.320 (6)	
$\Delta(v0-v2)$ (eV)	0.6335	···	0.670 (6)	
$\Delta(v0-v3)$ (eV)	0.9490	···	0.940 (6)	
Franck–Condon factors:				
$v0$	0.601		0.535	
$v1$	0.316		0.337	
$v2$	0.073		0.112	
$v3$	0.010		0.016	

[a] Reference 25.

[b] This work.

[c] Errors estimated from the results of several fits with different starting parameters.

[d] Assumed for calibration.

[e] Reference 25.

the equivalent-core and SCF (Hartree–Fock) approximations, but did not report the Franck–Condon factors. Gelius *et al.*[28] calculated the Franck–Condon factors of the ionized state using the empirical potential energy curves of ground state CO and NO^+, where the closed-shell NO^+ species is core equivalent to the $(C\ 1s^{-1})$ ionized state of CO. However there is poor agreement with results from vibrationally resolved $C\ 1s$ photoelectron spectra.[9,10] On the other hand, the present Franck–Condon factors for the $(C\ 1s^{-1})$ ionized state based on the CI potential energy are in good agreement with the recent experimental analysis.[9] The calculated vibrational spacing of 308 meV between the $v'=0$ and $v'=1$ states is also in good agreement with the photoelectron spectra [309 meV (Ref. 9), 301 meV (Ref. 10)] and the $(C\ 1s^{-1}$, Rydberg) photoabsorption spectra [292–307 meV (Ref. 8)]. It is marginally better than the result of the CASSCF and subsequent contracted CI calculations (322 meV)[26] and significantly better than the value of 330 meV based on the equivalent-core and SCF approximations.[29]

The difference in the singlet and triplet $(C\ 1s^{-1},\pi^*)$ states arises from the exchange interaction of the unpaired electrons in the $C\ 1s$ and π^* orbitals. Why should this give rise to a difference in potential curves? The smaller vibrational spacing in the $^3\Pi$ state implies a less tightly bound potential, consistent with the larger equilibrium bond distance and the larger Franck–Condon factors for the higher vibrational states. In CO, the π^* orbital is relatively strongly localized on the carbon atom. The greater ability of the trip-

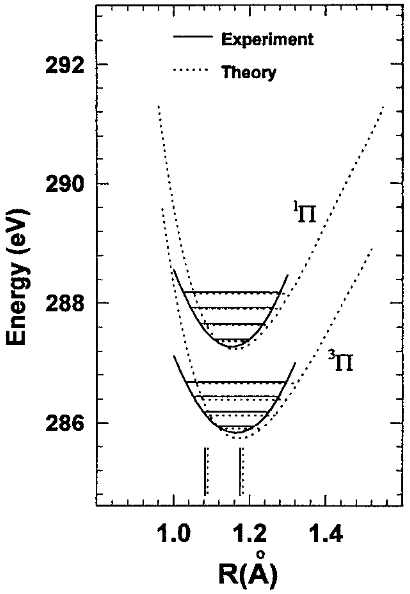

FIG. 5. Calculated anharmonic potential curves for the $(C\ 1s^{-1},\pi^*)\ ^3\Pi$ and $^1\Pi$ states compared to those estimated from the experimental results using an harmonic approximation. Each of the theoretical curves have been shifted 0.50 eV to lower energy. The vertical bars indicate the limits of the Franck–Condon region (the turning points of the $v=0$ level of the $X\ ^1\Sigma^+$ ground state) according to calculation (this work) and experiment (Ref. 25).

let electron configuration to allow the π^* and $C\ 1s$ electron to share the same region of space could lead to relatively greater π^* electron density at the carbon atom.

While it is dangerous to discuss bond length differences of 0.01 Å solely within a one-electron picture, in this case the Mulliken population and orbital contour analyses carried out in the one-electron (SCF) approximation which are summarized in Table II do give results consistent with the above. In particular they emphasize the importance of orbital relaxation in establishing the properties of the core excited states. While a more sophisticated CI analysis would likely make quantitative changes, the qualitative picture from the one-electron analysis appears reasonable. In the triplet state the "active charge transfer" (i.e., charge transfer to the core excited carbon atom involving the π^* electron) is twice as large as the "passive charge transfer" (i.e., rearrangement of the closed shell π and σ electrons) (see Table II). On the other hand, the active charge transfer by the π^* electron is smaller in the singlet state than in the triplet state so that the passive reorganization is relatively more important for the singlet state. Overall the relative effect of relaxation is that the unpaired π^* electron has more probability to be located at the carbon atom in the triplet state than in the singlet state. The ionized state has a shorter bond length because of greater Coulomb attraction between the C and O atoms relative to the ground state. The singlet excited state has nearly the same passive charge transfer as the ionized state. It is only the antibonding nature of the π^* orbital that elongates the bond in the singlet excited state. On the other hand, even though the antibonding nature of the π^* orbital is weaker in the triplet than the singlet excited state, the passive charge transfer is smaller in the triplet state (0.390) than in the ionized and singlet states (0.600, 0.648 respectively) and the Coulomb attraction arising in the passive charge transfer is weaker. This difference in relaxation is critical to establishing the difference between the potential energy curves in the singlet and triplet excited states.

TABLE II. Mulliken population analysis of charge and charge transfer calculated using the SCF orbitals for $R=1.160$ Å. The orbital relaxation is analyzed in the passive (closed-shell) and active (π^*) parts.

	Mulliken population	
State/charge transfer	C	O
Ground state	5.727	8.273
π^* orbital	0.809	0.191
Triplet state	5.894	8.106
π^* electron (active)	0.777	0.223
relaxation (passive)	+0.390	−0.390
total change	(+1.167−1.0)	−0.167
Singlet state	5.978	8.022
π^* electron (active)	0.604	0.396
relaxation (passive)	+0.648	−0.648
total change	(+1.251−1.0)	−0.251
Ionized state	5.327	7.673
relaxation (passive)	(+0.600−1.0)	−0.600
(total change)		

V. SUMMARY

In this work we have documented for the first time the angular dependence of a spin-forbidden core excitation. In addition, we have greatly extended the variable impact energy results of Harrison and King.[5,7] This study has given additional insight into the scattering mechanism and it has illustrated the breakdown of the Bethe–Born theory for slow collisional processes. High quality *ab initio* SCF-CI theoretical results have been reported and found to be in good agreement with the potential energy curves for the singlet and triplet $(C\ 1s^{-1},\pi^*)$ states derived from the experimental vibrational structure. The calculations illustrate the importance of orbital relaxation in establishing the details of core excited state potential curves.

ACKNOWLEDGMENTS

One of us (J.T.F.) acknowledges the Natural Science and Engineering Research Council (NSERC) for a research scholarship. We are deeply grateful to Dr. T. Tyliszczak for his assistance in the design and construction of the spectrometer and the data acquisition and analysis software, and to Dr. Shinkoh Nanbu for his advice and discussion of the molecular vibration and its numerical calculation.

[1] A. P. Hitchcock and D. C. Mancini, J. Electron Spectrosc. **67**, 1 (1994).
[2] D. A. Shaw, G. C. King, F. H. Read, and D. Cvejanović, J. Phys. B **15**, 1785 (1982).
[3] L. Ungier and T. D. Thomas, Chem. Phys. Lett. **96**, 247 (1983).
[4] D. A. Shaw, G. C. King, D. Cvejanović, and F. H. Read, J. Phys. B **17**, 2091 (1984).
[5] I. Harrison and G. C. King, J. Phys. B **19**, L447 (1986).
[6] J. T. Francis, C. Enkvist, S. Lunell, and A. P. Hitchcock, Can. J. Phys. (in press).

[7] I. Harrison, Ph. D. Thesis, University of Manchester, 1986; I. Harrison and G. C. King, J. Electron Spectrosc. **43**, 155 (1987).

[8] M. Domke, C. Xue, A. Puschmann, T. Mandel, E. Hudson, D. A. Shirley, and G. Kaindl, Chem. Phys. Lett. **174**, 668 (1990); **173**, 122 (1990).

[9] L. J. Medhurst, P. A. Heinmann, M. R. F. Siggel, D. A. Shirley, C. T. Chen, Y. Ma, S. Modesti, and F. Sette, Chem. Phys. Lett. **193**, 493 (1992).

[10] K. J. Randall, A. L. D. Kilcoyne, H. M. Koppa, J. Feldhaus, A. M. Bradshaw, J. E. Rubensson, W. Eberhardt, Z. Xu, P. D. Johnson, and Y. Ma, Phys. Rev. Lett. **71**, 1156 (1993).

[11] Y. Ma, F. Sette, G. Meigs, S. Modesti, and C. T. Chen, Phys. Rev. Lett. **63**, 2044 (1989).

[12] Y. Ma, F. Sette, G. Meigs, S. Modesti, and C. T. Chen, Phys. Scr. **41**, 833 (1990); Y. Ma, C. T. Chen, G. Meigs, K. Randall and F. Sette, Phys. Rev. A **44**, 1848 (1991).

[13] N. Kosugi and H. Kuroda, Chem. Phys. Lett. **74**, 490 (1980).

[14] N. Kosugi, Theor. Chim. Acta **72**, 149 (1987).

[15] Y. Yagishita, E. Shigemasa, and N. Kosugi, Phys. Rev. Lett. **72**, 3961 (1994).

[16] S. Iwata and N. Sato, J. Chem. Phys. **82**, 2346 (1985).

[17] J. W. Cooley, Math. Comput. **15**, 363 (1961).

[18] S. Iwata, N. Kosugi, and O. Nomura, Jpn. J. Appl. Phys. **17**, Suppl. 2, 109 (1978).

[19] S. Huzinaga, J. Andzelm, M. Kłobukowski, E. Radzio-Andzelm, Y. Sakai, and H. Tatewaki, *Gaussian Basis Sets for Molecular Calculations* (Elsevier, Amsterdam, 1984).

[20] E. N. Lassettre and A. Skerbele, in *Methods of Experimental Physics*, edited by D. Williams, Vol. 3 (Part B), Chap. 7.2, 868 (Academic, New York, 1974).

[21] M. Inokuti, Rev. Mod. Phys. **43**, 297 (1971).

[22] D. M. Cooper and S. R. Langhoff, J. Chem. Phys. **74**, 1200 (1981).

[23] E. N. Lasettre and M. A. Dillon, J. Chem. Phys. **59**, 4778 (1973).

[24] M. A. A. Clyne and M. C. Heaven, J. Chem. Soc. Faraday Trans. 2 **77**, 1375 (1981).

[25] G. Herzberg and K. P. Huber, *Constants of Diatomic Molecules* (Van Nostrand Reinhold, New York, 1979).

[26] N. Correia, A. Flores-Riveros, H. Ågren, K. Helenelund, L. Asplund, and U. Gelius, J. Chem. Phys. **83**, 2035 (1985).

[27] H. Ågren, L. Selander, J. Nordgren, C. Nordling, K. Siegbahn, and J. Müller, Chem. Phys. **37**, 161 (1979).

[28] U. Gelius, S. Svensson, H. Siegbahn, E. Basilier, Ä. Faxälv, and K. Siegbahn, Chem. Phys. Lett. **28**, 1 (1974).

[29] T. D. Clark and J. Müller, Theor. Chim. Acta **41**, 193 (1976).